Integrated Silicon Photovoltaics on CMOS With MEMS Module for Catheter Tracking

Mohammad Hossein Mazaheri Kouhani, Berk Camli, Ahmet Uraz Cakaci, Emre Kusakci, Baykal Sarioglu, Gunhan Dundar, Hamdi Torun, and Arda Deniz Yalcinkaya, *Member, IEEE*

***Abstract*—This paper presents an electromagnetic actuation-based optoelectronic active catheter tracking system for magnetic resonance imaging (MRI). The system incorporates a radio frequency (RF) microelectromechanical system (MEMS) resonator array actuated by the Lorentz force induced due to the strong dc magnetic field available in MRI environment. Power transfer to the system and the actuation detection are done optically via fiber optic cables that replace conventional conductive transmission lines; thereby, enabling the tracking system to function safely under MRI. The complementary metal–oxide–semiconductor (CMOS) receiver, optically powered by a supply unit housing an on-chip silicon photovoltaic cell, detects the location of the catheter tip. The RF MEMS resonator array transmits the position data by transducing the electrical signal into a resonant mechanical vibration linearly. The optical reading of this actuation can be done by diffraction grating interferometry or laser doppler vibrometry. The fabricated resonator array is tested with the optically powered CMOS chip (0.18-μm UMC technology) in laboratory conditions. The driving electrical current supplied by the chip for resonator actuation is 25-μA rms, where the magnetic field provided by the experimental setup is 0.62 T. The resonator array is observed to be functional with real-world application by showing a frequency response of 10 dB, which will be enhanced further under the stronger magnetic field available in 3-T MRI.**

***Index Terms*—Catheter tracking, complementary metal–oxide–semiconductor (CMOS), electromagnetic actuation, magnetic resonance imaging (MRI), microelectromechanical system (MEMS), silicon photovoltaics.**

I. Introduction

LOCALIZATION of endovascular catheters are of great importance in minimally invasive medical operations. Major types of imaging platforms for such operations are X-ray fluoroscopy (XF), sonography, and magnetic resonance imaging (MRI). XF is associated with high doses of ionizing radiation that is potentially harmful to the patient and the medical staff [1]; whereas sonography suffers from a limited field of view [2]. A promising platform which provides a safe environment with a high soft-tissue contrast is MRI [3].

MRI is based on the principle that in a constant magnetic field, nuclear magnetic dipoles resonate at a frequency linearly related to the magnitude of the dc magnetic field. Dipoles excited by an additional superimposed ac electromagnetic pulse at this frequency respond by emitting free induction decay (FID) signals as they return to their stable states. Localization of each FID source can be done by grading the magnitude of the strong magnetic field across the physical dimension so that each point in that dimension is assigned a particular resonant frequency. Grading should be high enough to allow the separation of two signals and low enough so that nuclei with shifted resonant frequencies can still be excited through the ac pulse. The principle that MRI resolves the localization issue by mapping position to frequency forms a basis for many catheter tracking systems.

The majority of existing MRI tracking systems use electrical conductors for signal and power transmission [4], [5]. However, the strong radio frequency (RF) pulses in MRI bear the risk of heat induction in conductive materials [6]. A number of techniques have been employed to reduce the induction of heat in endovascular catheters; such as utilizing coaxial chokes [6], exerting resonance frequency shift [7], and optical methods using fiber optic cables [8], [9]. In [8], excessively high concentration of energy on a single spot is mentioned as a potential challenge for optical tracking. In [9] Fandrey *et al.* used a special discrete photovoltaic power converter and a discrete laser diode with a JFET for signal processing in MRI. However, these techniques incorporate optoelectronic components that can not be monolithically integrated with the signal processing electronics. To address these issues, we propose a system with following two major novelties: i) the utilization of fiber optic cables for data and power transmission that is enabled by the integration of silicon photovoltaics on complementary metal–oxide–semiconductor (CMOS) and ii) incorporation of a MEMS-based resonator array as the off-chip electronics/optics interface component reducing the power consumption significantly compared to previous optically communicating systems [10].

MEMS technology has been utilized in lightwave communication for more than three decades [11]. MEMS-based packages have been demonstrated, for vertical-cavity surface emitting lasers [12]. In addition, movable apertures and reflectors have been developed using MEMS technology for a variety of applications [13]–[19]. As an optical switch, [13] presents

Manuscript received October 31, 2014; revised January 13, 2015; accepted January 15, 2015. Date of publication February 4, 2015; date of current version July 13, 2015. This work was supported in part by the Technological Research Council of Turkey (TÜBİTAK) under Project EEEAG 111E197. The work of A. D. Yalcinkaya was supported in part by the Turkish National Academy of Sciences Distinguished Young Scientist Award Program (TUBA GEBIP).

M. H. Mazaheri Kouhani, B. Camli, A. U. Cakaci, E. Kusakci, and G. Dundar are with the Department of Electrical and Electronics Engineering, Bogazici University, TR-34342 Istanbul, Turkey (e-mail: hossein.mazaheri@boun.edu.tr; berk.camli@boun.edu.tr; aucakaci@gmail.com; emre.kusakci@gmail.com; dundar@boun.edu.tr).

B. Sarioglu was with the Department of Electrical and Electronics Engineering, Bogazici University, TR-34342 Istanbul, Turkey. He is now with the Department of Electrical and Electronics Engineering, Bilgi University, Eyup, TR-34060, Turkey (e-mail: baykal.sarioglu@bilgi.edu.tr).

H. Torun and A. D. Yalcinkaya are with the Department of Electrical and Electronics Engineering and the Center for Life Sciences and Technologies, Bogazici University, TR-34342 Istanbul, Turkey (e-mail: hamdi.torun@boun.edu.tr; arda.yalcinkaya@boun.edu.tr).

Color versions of one or more of the figures in this paper are available online at http://ieeexplore.ieee.org.

Digital Object Identifier 10.1109/JLT.2015.2396117

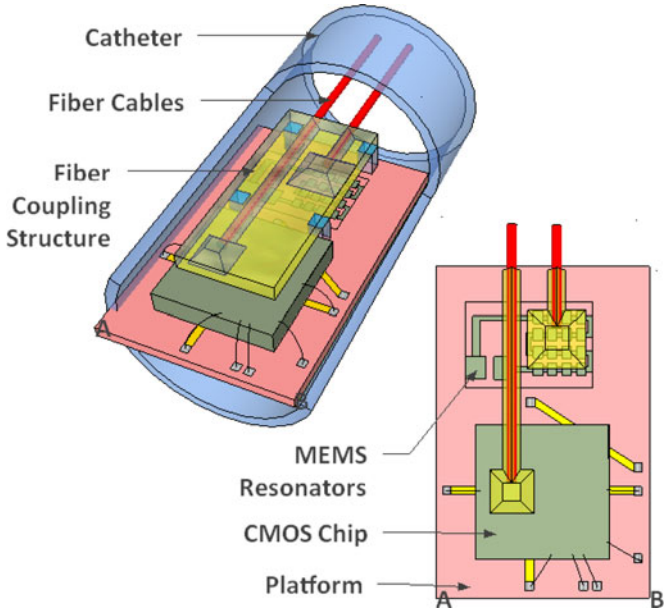

Fig. 1. General representation of the tracking microsystem fit in a catheter.

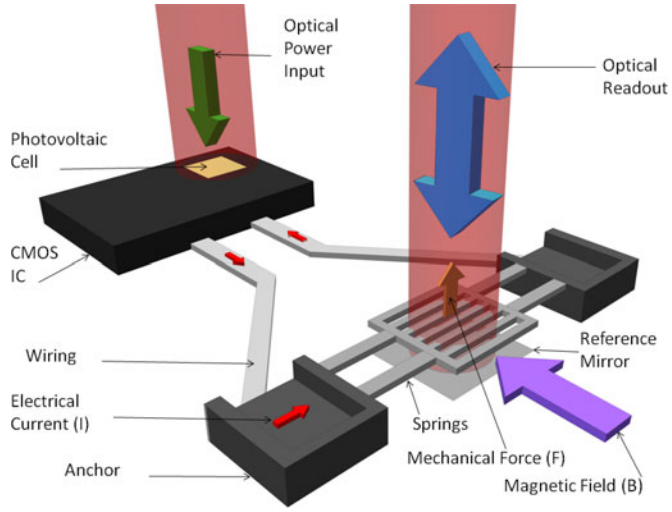

Fig. 2. Main system blocks and representation of MEMS resonator actuation mechanism. Note that the application of diffraction grating interferometry technique would require a reference mirror beneath the resonator structure.

a physical-parameter design of a 2-D switch used for all-optical cross connects. Also, in [16], vertical torsion mirrors are utilized for free-space fiber-optic switches. Electrothermal MEMS actuators are used in variable optical attenuators by controlling the size of an aperture formed by electrothermally movable blades [17] or moving the location of a pair of MEMS reflectors [14]. For optical bandpass filter realization, a variable-aperture MEMS reflector is utilized in [15]. Magnetic actuation can also be realized as in [18] for a swing-type MEMS mirror, which is used for a reconfigurable optical interconnect. Optical read-out methods are also of great utility in detecting the deflection of MEMS cantilevers and resonators. For instance, [19] proposes an optical read-out method based on interferometers suitable for cantilever sensor array.

This work presents a tracking system, which consists of a CMOS chip and an off-chip MEMS resonator array, communicating with the outside world via optical interfaces. The integrated system fits in a catheter as depicted in Fig 1. This paper is organized as follows: Section II describes the system elements and their design including the simulation and microfabrication of the MEMS resonators. Section III presents the experimental characterization results and Section IV concludes this work.

II. System Description and Design

The CMOS chip detects and processes the input FID signals while being powered by a power supply unit based on a silicon photovoltaic cell converting the optical input power carried by a fiber optic cable. The on-chip receiver modulates the output of a current source, which drives the array of MEMS resonators in accordance with the position-frequency duality. This results in a Lorentz force on the resonators under the presence of the strong dc magnetic field of the MRI environment. The actuation is linearly related to current, so the response is at the same frequency as the PWM current signal. The frequency of the vibration is detected by optical means via a second fiber optic cable.

A. CMOS Chip

The on-chip current source regulated by the receiver was designed to supply a current of 25 μA rms when a supply of 0.8 V or higher is available. An improvement associated with the reduced power requirements of the presented system is that the CMOS chip can be powered continuously, removing any requirements of synchronization with the MRI.

The central element of the supply unit is the integrated silicon photovoltaic cell of 1.21 mm^2 footprint area. The fact that it is formed of p-n junctions available in CMOS technology introduces further flexibility in terms of system integration. The supply unit is complete with a dc/dc converter block utilized to increase the voltage provided by the silicon photovoltaic cell so that the receiver can be supplied properly. An off-chip storage capacitor of 100 nF is also required for supply stability [20].

A direct conversion self-mixing architecture is implemented for the receiver. The receiver is designed to downconvert the MRI signals within the 120 MHz band to the baseband with a cutoff frequency of 1 MHz.

B. MEMS Resonator Structure and Simulation

A family of resonators with various geometries is designed to enhance the detection resolution of localization signals. Typically, a single resonator is a double-clamped movable metallic beam having either one or two springs on each side holding either a diffraction grated mirror (55 μm $\times$ 60 μm) or a square-perforated mirror (40 μm $\times$ 40 μm) in the centers. Length and/or width of the springs change from one resonator to another. The variance in the geometry of resonators results in the variance of their resonance frequency. The thickness of all the resonators is 1.5 μm and the gap between the mirror and the substrate is 3.2 μm.

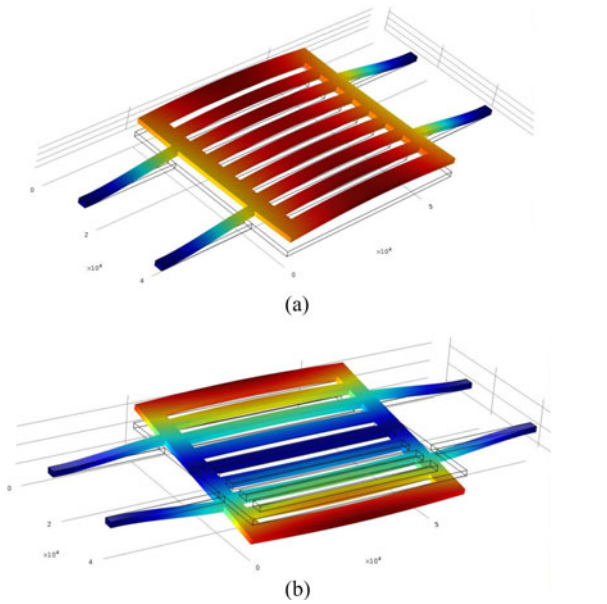

Fig. 3. Mode analysis simulations of a resonator. (a) Out-of-plane mode ($f = 325$ kHz) and (b) torsional mode ($f = 379$ kHz).

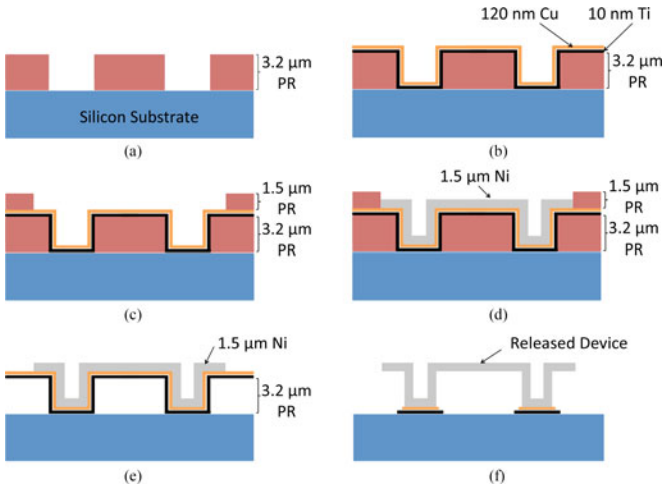

Fig. 4. The fabrication sequence of the MEMS resonator in side view. (a) Photolitography 1, (b) sputtering of titanium and copper, (c) photolithography 2, (d) electroplating nickel, (e) releasing, (f) wet etching.

The metallic structural layer of the resonator is an electrically conductive path for the current provided by the CMOS chip. This results in out-of-plane deflection in presence of an electric current within a magnetic field due to the Lorentz force expressed by the relation:

$$\vec{\mathbf{F}} = I\vec{\mathbf{l}} \times \vec{\mathbf{B}} \tag{1}$$

where $\vec{\mathbf{F}}$ is the vector quantity of Lorentz force, I is the current passing through the structure, $\vec{\mathbf{l}}$ is the direction vector of magnitude equal to the length of the structure, and $\vec{\mathbf{B}}$ is the magnetic field vector. Fig. 2 shows the integration of the MEMS resonator with CMOS IC and illustrates the actuation mechanism. The electromagnetic force interacts with the mechanical device, which has an effective stiffness of k, to result in the out-of-plane deflection of the MEMS mirror. Magnitude of the mirror deflection at resonance, Δz, can be approximated as

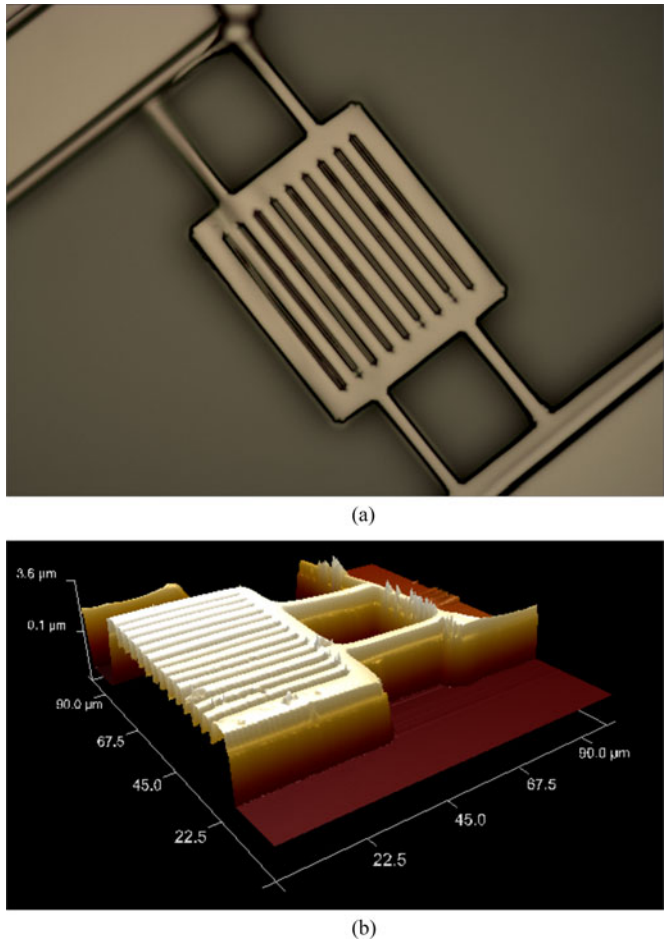

Fig. 5. (a) Micrograph of a released device in top view. (b) Topographic image of the device obtained using an atomic force microscope.

$$\Delta z \approx \frac{F}{k} Q \tag{2}$$

where F is the magnitude of the mechanical force vector normal to the mirror and Q is the mechanical quality factor of the MEMS device.

Mode analysis of a specific design using finite element method (FEM)-based simulations are shown in Fig. 3. Here, Fig. 3(a) shows the first mode of the device at 325 kHz exhibiting out-of-plane motion; whereas Fig. 3(b) shows the second mode of the device. The device exhibits torsional motion in the second mode where the center of the mirror is stationary. Contribution of this second mode is not significant since the read-out method is sensitive only to out-of-plane motion.

C. Microfabrication of the MEMS Resonator

The fabrication process is formed of a simple two-mask surface micromachining. First, a photolithography step defines the sacrificial layer as shown in Fig. 4(a), which is a 3.2 μm thick photoresist layer. Then, a seed layer of 120 nm thick copper is

TABLE I
SIMULATED AND MEASURED RESONANCE FREQUENCIES, QUALITY FACTORS, THE RELATED CURRENT CONSUMPTION, AND THE GEOMETRY OF THE TESTED RESONATORS

Resonator #	Sim. / Meas. Resonant Frequency (kHz)	Quality Factor	PWM Current (μA rms)	Spring L/W (μm)	Number of Springs
1	268/325	35	25	45/2.5	2
2	325/402	77.3	3800	30/5	1
3	417/435	87.1	360	32/2.5	2
4	431/502	143.4	250	26/3	1
5	535/575	192	4500	26/2.5	2
6	624/635	127	3800	20/4	1
7	645/710	88.7	4500	22/2.5	2
8	751/805	115	4500	19/2.5	2

sputtered on top after a layer of 10 nm thick titanium is used as an adhesion promoter as depicted in Fig. 4(b).

The second photolithography step defines the masking layer for electroplating as in Fig. 4(c). A 1.5 μm thick nickel layer is electroplated to define the structural layer using a sulfamate bath as demonstrated in Fig. 4(d). Oxygen plasma is utilized to release the devices as shown in Fig. 4(e). As the last step, copper and titanium layers are etched away from beneath the beams as in Fig. 4(f). A micrograph and a 3-D topographic image of a released device obtained using an atomic force microscope are presented in Fig. 5.

III. EXPERIMENTAL CHARACTERIZATION

The CMOS was fabricated using 0.18 μm UMC technology with a die area of 1525 μm $\times$ 1525 μm. To test resonators as they are driven by the CMOS IC, optical fibers are coupled to the test chips for operational stability. Coupling is performed in macroscale using structures which are manufactured by stereolithography. The couplers are essentially cubic structures of 1.2 cm unit length, allowing them to be easily mounted on the chip packaging without interfering with the chip itself and the wire bonds directly. Mounting is realized such that a cylindrical hole of 1 mm diameter perforating the holder body is axially aligned with the center of the silicon photovoltaic cell. A fiber fixed to a 3-D stage was then put through the cylindrical hole. Position of the fiber was adjusted via the 3-D stage as a laser beam was continually being transmitted to the photovoltaic cell through the fiber and the open circuit voltage of the photovoltaic cell was being observed. A laser source of 650 nm wavelength with adjustable output power up to 80 mW (Coherent CUBE 660-75 FP) was used for the coupling procedure as well as all the other optical powering procedures described in this work. The fiber was fixed into its position within the hole with the application of some adhesive epoxy after an optimal response point was obtained.

Absolute loss in short circuit current of the photovoltaic cell due to coupling is around 0.32 mA, if data of [20] are considered as a reference for non-coupled photovoltaic cell performance. This corresponds to relative loss values of 3.4% and 13.8% for 80 and 30 mW of laser power. Measurements showed that this translates to relative loss values of 3.1% and 23.2% at 80 and 30 mW, respectively, for the short circuit current of the overall supply unit.

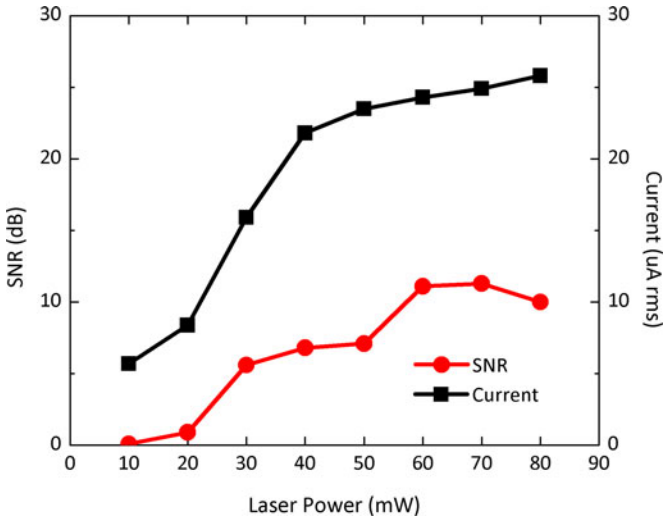

Fig. 6. The change in SNR and the rms value of the PWM current for varying laser power levels.

Coupled CMOS chips were then used to drive the MEMS resonators. While the laser source continues to power the chip, the analog inputs are provided by a signal generator (Rohde & Schwarz SMB 100A) and a function generator (Tektronix AFG 3251C). The resonators connected to the CMOS chip through a 500 Ω series resistor were mounted between two cubic N48 magnets placed one inch apart. Flux density of the magnetic field formed between the magnets was measured to be 0.62 T. The resonators were characterized using a laser Doppler vibrometer (Polytec OFV-2500) and a spectrum analyzer (Rohde & Schwarz FSV40) to observe the output signal-to-noise ratio (SNR). Waveshape of the PWM signal provided by the chip is observed indirectly for verification purposes. This was done by probing the voltage across the series resistor with a classical three-OPAMP unity gain instrumentation amplifier made of discrete components to prevent loading. Output of the amplifier was observed using an oscilloscope. A multimeter was also used to record the rms value of the current as well.

Tested resonators are numbered from 1 to 8. Resonator 2 has a diffraction grated mirror and the rest of the resonators have square-perforated mirrors. Their characteristics and relevant measurement results are shown in Table I. Two sets of measurements are done with a single resonator (shown as Resonator 1 in Table I) having a measured resonance frequency of 325 kHz. During the measurements, the output SNR and the driving rms current are recorded. The first set of measurements were taken when both signal amplitudes were fixed at -50 dBm (frequencies are set to 120.000 and 120.325 MHz) while the laser power level was swept. Results regarding these measurements are presented in Fig. 6. Results indicate that a measurable current exists at laser power levels as low as 30 mW.

For the second set of measurements, the signal amplitudes were swept this time while the laser power was kept constant

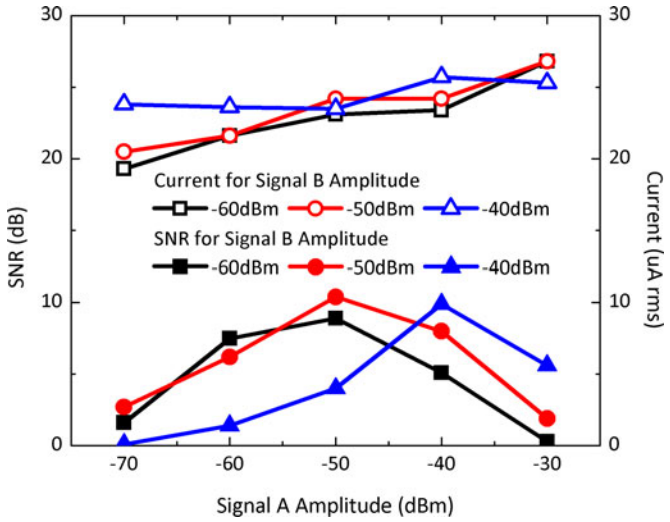

Fig. 7. The change in SNR and the rms value of the PWM current for varying input signal levels.

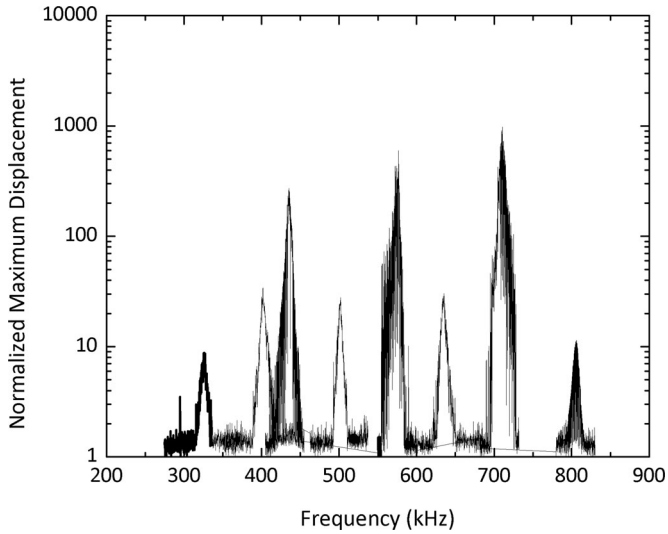

Fig. 8. The frequency response of a family of eight resonators with different geometries and resonant frequencies.

at 60 mW. Other conditions being the same, data shown in Fig. 7 are obtained. Since signals with significantly different amplitudes create a more prominent dc component after self-mixing, SNR is more favorable when the input levels are close to each other. In addition, increasing input levels increase the rms amplitude of the generated current.

Out-of-plane motions of the eight members of an array of MEMS resonators driven by the CMOS chip were observed by the LDV and the spectrum analyzer setup. Frequency of the MEMS resonator drive current carries the catheter position information in MRI. The MEMS device generates a displacement at the same frequency of the drive current. Frequency of the displacement can then be utilized as a measure to extract the relative position of the catheter, through frequency-encoding technique as given in [2]. Displacement spectrum obtained by the superposition of the individual device spectra are presented in Fig. 8. The spectrum is normalized to unity at off-resonance.

Simulated and measured resonant frequencies, quality factors, and the driving currents used for the characterization of each resonator are tabulated in Table I. Resonator 1 is characterized while it is supplied by the CMOS chip directly, drawing a current of 25 μA rms. For the other resonators, the PWM current is amplified by an external low noise transimpedance amplifier. These resonators yielded larger SNR values. The magnetic field of 0.62 T, available in the current characterization setup is nearly five times lower than the one in 3 T MRI environment. Therefore, the SNR value of 10 dB measured for Resonator 1 is expected to be larger in MRI. The minimum detectable value of the maximum displacement is measured to be 50 pm. The absolute value of maximum displacement for the resonator 1 with respect to PWM frequency is presented in Fig. 9.

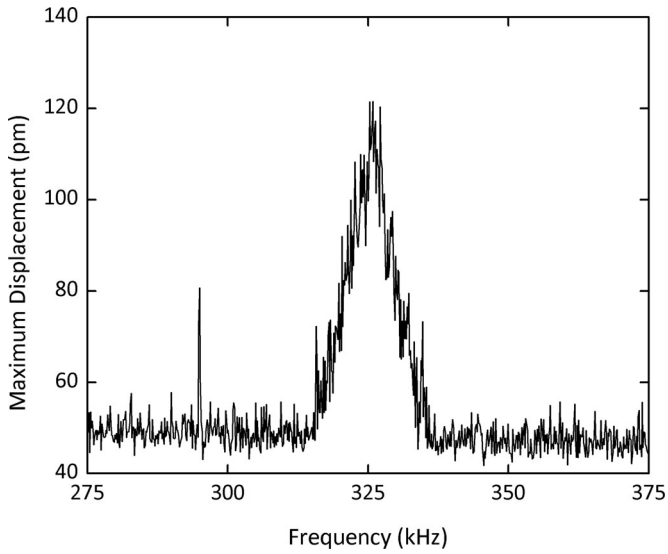

Fig. 9. Maximum displacement of resonator 1 observed within the frequency band around the resonance frequency.

IV. Conclusion

In this work, an electromagnetic catheter tracking system is presented. The tracking circuitry is a CMOS chip powered optically by an integrated silicon photovoltaic cell. Under MRI, the receiver unit in the chip detects the FID signals with a micro-coil antenna and generates a PWM electrical current. An array of RF MEMS resonators is incorporated to the interface between optics and electronics. The resonator deflects due to induced Lorentz force linearly at the frequency of PWM. The movable part of the resonator is patterned by diffraction gratings, enabling the detection of vibration using diffraction grating interferometry or laser Doppler vibrometry.

The resonators were fabricated by electroplating nickel on a silicon substrate via a simple two-mask surface micromachining. The fabricated devices were characterized using an optical characterization setup. The experimentally obtained resonant frequencies of resonators are in good agreement with FEM simulation results with a maximum relative error of 23.7%.

The CMOS chip was fabricated using 0.18 μm UMC technology along with silicon photovoltaic cells formed of the p-n junctions available in the process. A feasible method for the chip to be able to operate with the resonator array is the permanent coupling of a fiber cable to the chip. In this work, the coupling performed without the use of sophisticated equipment. Nevertheless, the constant loss introduced due to coupling can be considered insignificant at sufficiently high laser power levels. The relative loss is as low as 3.1% when the laser power is set to 80 mW. PWM current generation performance indicate that the CMOS chip is still operational below a laserr power of 30 mW while yielding relatively lower SNR values. Above 60 mW no significant change in SNR performance is observed.

The system consisting of the chip and the resonator array operates successfully over a wide range of laser power and input signal amplitude levels. Resonator 1 can be actuated even when the magnetic field generated in the laboratory is five times lower than a 3 T MRI machine. For the other resonators, a transimpedance amplifier was used to amplify the driving current to the resonator and obtain higher SNR values.

In the future, components of the system will be integrated on a platform that could be mounted or fit into a catheter. The photovoltaic cell and the receiver cover 1.05 and 0.3 mm^2, respectively, whereas the whole die covers an area of 2.33 mm^2. A single array of MEMS resonators is quite small compared to the CMOS chip and thus can easily be integrated with without increasing system size. So it is possible to incorporate even more resonators for more uniform frequency response. The challenge is alleviated by the fact that the system does not require too many communication paths and wire-bonds to be added or patterned on the platform. The system will be operational as it will be fed with a laser at a power level of 40 mW at its output. The system supplied by the optical power source is able to operate with 2 mW of power. The overall module could fit into an 8-Fr catheter compatible with intravascular interventions.

REFERENCES

[1] M. Vlaardingerbroek, J. den Boer, and E. Haacke, "Magnetic resonance imaging: Theory and practice," *Amer. J. Roentgenol.*, vol. 168, no. 3, pp. 656–656, 1997.

[2] D. A. Leung, J. Debatin, S. Wildermuth, G. McKinnon, D. Holtz, C. Dumoulin, R. Darrow, E. Hofmann, and G. Von Schulthess, "Intravascular MR tracking catheter: Preliminary experimental evaluation," *Amer. J. Roentgenol.*, vol. 164, no. 5, pp. 1265–1270, 1995.

[3] R. A. Kleinerman, "Cancer risks following diagnostic and therapeutic radiation exposure in children," *Pediatr. Radiol.*, vol. 36, no. 2, pp. 121–125, 2006.

[4] C. M. Hillenbrand, D. R. Elgort, E. Y. Wong, A. Reykowski, F. K. Wacker, J. S. Lewin, and J. L. Duerk, "Active device tracking and high-resolution intravascular MRI using a novel catheter-based, opposed-solenoid phased array coil," *Magn. Reson. Med.*, vol. 51, no. 4, pp. 668–675, 2004.

[5] R. D. Darrow, C. L. Dumoulin, J. F. Schenck, and S. P. Souza, "Tracking system to follow the position and orientation of a device with radiofrequency field gradients," U.S. Patent 5 211 165, May 18, 1993.

[6] M. E. Ladd and H. H. Quick, "Reduction of resonant RF heating in intravascular catheters using coaxial chokes," *Magn. Reson. Med.*, vol. 43, no. 4, pp. 615–619, 2000.

[7] S. Weiss, P. Vernickel, T. Schaeffter, B. Gleich, and V. Schulz, "Towards an RF-safe active catheter for MR-guided interventions," *Medica Mundi*, vol. 49, no. 3, pp. 48–53, 2005.

[8] M. Konings, S. Weiss, C. Bakker, L. Bartels, and W. Mali, "Catheters and guidewires in interventional MRI: Problems and solutions," *Medicamundi*, vol. 45, no. 1, pp. 31–39, 2001.

[9] S. Fandrey, S. Weiss, and J. Muller, "Development of an active intravascular MR device with an optical transmission system," *IEEE Trans. Med. Imag.*, vol. 27, no. 12, pp. 1723–1727, Dec. 2008.

[10] B. Sarioglu, O. Aktan, A. Oncu, S. Mutlu, G. Dundar, and A. Yalcinkaya, "An optically powered CMOS receiver system for intravascular magnetic resonance applications," *IEEE J. Emerging Sel. Topics Circuits Syst.*, vol. 2, no. 4, pp. 683–691, Dec. 2012.

[11] M. C. Wu, O. Solgaard, and J. E. Ford, "Optical MEMS for lightwave communication," *J. Lightw. Technol.*, vol. 24, no. 12, pp. 4433–4454, Dec. 2006.

[12] A. K. Nallani, T. Chen, D. J. Hayes, W.-S. Che, and J.-B. Lee, "A method for improved VCSEL packaging using MEMS and ink-jet technologies," *J. Lightw. Technol.*, vol. 24, no. 3, pp. 1504–1512, Mar. 2006.

[13] L. Savastano, G. Maier, A. Pattavina, and M. Martinelli, "Physical-parameter design in 2-D MEMS optical switches," *J. Lightw. Technol.*, vol. 23, no. 10, pp. 3147–3155, Oct. 2005.

[14] C. Lee, "A MEMS VOA using electrothermal actuators," *J. Lightw. Technol.*, vol. 25, no. 2, pp. 490–498, Feb. 2007.

[15] K. Yu, D. Lee, N. Park, and O. Solgaard, "Tunable optical bandpass filter with variable-aperture MEMS reflector," *J. Lightw. Technol.*, vol. 24, no. 12, pp. 5095–5102, Dec. 2006.

[16] S.-S. Lee, L.-S. Huang, C.-J. Kim, and M. C. Wu, "Free-space fiber-optic switches based on MEMS vertical torsion mirrors," *J. Lightw. Technol.*, vol. 17, no. 1, pp. 7–13, Jan. 1999.

[17] H. Veladi, R. R. Syms, and H. Zou, "Fiber-pigtailed electrothermal MEMS iris VOA,"*J. Lightw. Technol.*, vol. 25, no. 8, pp. 2159–2167, Aug. 2007.

[18] C.-W. Tsai, H.-T. Chang, S.-H. Liu, and J.-C. Tsai, "Magnetically-actuated swing-type MEMS mirror pair for a reconfigurable optical interconnect," *J. Lightw. Technol.*, vol. 31, no. 24, pp. 4126–4134, Dec. 2013.

[19] G. Putrino, A. Keating, M. Martyniuk, L. Faraone, and J. Dell, "Model and analysis of a high sensitivity resonant optical read-out approach suitable for cantilever sensor arrays," *J. Lightw. Technol.*, vol. 30, no. 12, pp. 1863–1868, Jun. 2012.

[20] B. Camli, B. Sarioglu, and A. Yalcinkaya, "Photodiodes for monolithic CMOS circuit applications," *IEEE J. Sel. Topics Quantum Electron.*, vol. 20, no. 6, Nov./Dec. 2014.

Mohammad Hossein Mazaheri Kouhani was born in Tehran, Iran, in 1988. He received the B.Sc. degree from the University of Tehran, Tehran, in 2012, and the M.Sc. degree from Bogazici University, Istanbul, Turkey, in 2014, both in electrical and electronics engineering, where he is currently working toward the Ph.D. degree at the Biomedical Engineering Institute. His current research interests include implantable biomedical microdevices, neural interfaces, micro/nanosensors and actuators, bioMEMS/NEMS, and microfluidics

Berk Camli was born in Ankara, Turkey in 1987. He received the B.S.(Hons.) and M.S. degrees in electrical engineering from Bogazici University, Istanbul, Turkey, in 2010 and 2013, respectively, where he is currently working toward the Ph.D. degree. He is currently a Research Assistant with the Bogazici University, focusing on microsystem design for biomedical applications. He received the Turkish Prime Ministry Scholarship (2005–2010), and Is Bankasi Golden Youth Award in 2005.

Ahmet Uraz Cakaci received the B.Sc. and M.Sc. degrees in electrical and electronics engineering from Bogazici University, Istanbul, Turkey, in 2010 and 2013, respectively. He is currently working toward the Ph.D. degree in electrical and electronics engineering at Middle East Technical University, Ankara, Turkey. He was a Member of Prof. Yalnkayas Research Group from 2011 to 2013 and contributed to the MEMS resonators design and fabrication. He is currently working as an R&D Engineer at Aselsan Inc., Ankara. His current technical research interests include design of radar systems and algorithms.

Emre Kusakci received the B.S.(Hons.) degree in electrical & electronics engineering and physics from Bogazici University, Istanbul, Turkey, in 2013, where he is currently working toward the master's degree. He is currently a Teaching Assistant with Bogazici University. His research interests include photonics, design, fabrication, and characterization of MEMS devices, CMOS-MEMS integration, and metamaterials. He received the Turkish Prime Ministry Fellowship (2008–2013) and Nortel Networks Netas Telecommunication Fellowship (2012–2013).

Baykal Sarioglu received the B.S. degree(Hons.) from Kadir Has University, Istanbul, Turkey, in 2004, and the M.Sc. and Ph.D. degrees from Bogazici University, Istanbul, in 2007 and 2013, respectively, all in electrical engineering . He is currently an Assistant Professor at the Department of Electrical Engineering, Bilgi Universty, Beyoglu, Turkey. His research interest includes analog ASIC design for biomedical applications.

Gunhan Dundar was born in Istanbul, Turkey, in 1969. He received the B.S. and M.S. degrees from Bogazici University, Istanbul, in 1989 and 1991, respectively, and the Ph.D. degree from the Rensselaer Polytechnic Institute, Troy, NY, USA, in 1993, all in electrical engineering .

In 1994, he was a Lecturer with Bogazici University, teaching courses on electronics, electronics laboratory, IC design, electronic design automation, and semiconductor devices. From August 1994 to November 1995, he was with the Turkish Navy and taught courses on electronics, electronics laboratory, and signals and systems with the Turkish Naval Academy, Istanbul. Since 1995, he has been with Bogazici University, where he is currently a Professor. Between 2006 and 2009, he was the Chairman of the Department of Electrical and Electronics Engineering. Between 2002 and 2003, he was with the cole Polytechnique Fdrale de Lausanne, Lausanne, Switzerland, and between 2009 and 2010, he was with the Technical University of Munich, on sabbatical leave. His research interests include analog integrated-circuit design, computer-aided design for analog design, and soft-computing circuits.

Hamdi Torun received the B.S. degree from Middle East Technical University, Ankara, Turkey, in 2003, the M.S. degree from Ko University, Istanbul, Turkey, in 2005, and the Ph.D. degree from the Georgia Institute of Technology, Atlanta, GA, USA, in 2009, all in electrical engineering. He was a Postdoctoral Fellow with the Department of Mechanical Engineering, Georgia Institute of Technology, during 2009 to 2010. He is currently an Assistant Professor at the Department of Electrical and Electronics Engineering and affiliated with the Center for Life Sciences and Technologies, Bogazici University, Istanbul. His research interest includes development of microsystems for biomedical applications.

Arda Deniz Yalcinkaya (S'96–M'06) received the B.S. degree from the Electronics and Telecommunication Engineering Department, Istanbul Technical University, Istanbul, Turkey, and the M.Sc. and Ph.D. degrees from the Department of Micro and Nano Technology, Technical University of Denmark, Kgs. Lynby, Denmark, in 1997, 1999, and 2003, respectively, all in electrical engineering.

Between 1999 and 2000, he was a Research and Development Engineer with Aselsan Microelectronics, Ankara, Turkey. He was a Visiting Researcher with Interuniversity Microelectronic Center, Leuven, Belgium, and Centro Nacionale de Microelectronica, Barcelona, Spain, in 2000 and 2003, respectively. Between 2003 and 2006, he was a Postdoctoral Research Associate with Koc University, Istanbul. During that period, he served as a Consultant with Microvision Inc., Seattle, USA. Since 2006, he has been a Faculty Member with the Department of Electrical and Electronics Engineering, Bogazici University, Istanbul, where he is currently an Associate Professor. His research interests include photonics, metamaterials, microelectromechanical systems, and analog integrated circuits. He received the Sabanci Foundation (VAKSA) Turkish Education Foundation scholarships during his studies. He received the Bogazici University Foundation Excellence in Research Award, the Middle East Technical University Mustafa Parlar Foundation Research Encouragement Award and Turkish Academy of Sciences, the Distinguished Young Scientists Award (GEBIP) in 2010, 2011, and 2013, respectively.